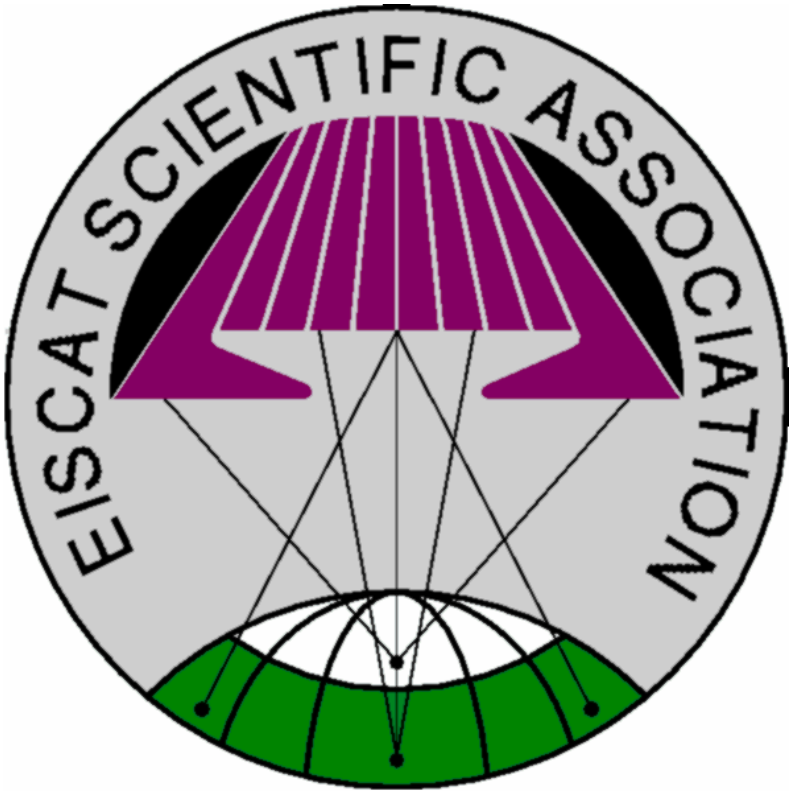

EISCAT TECHNICAL REPORT 09/57

WAVE POLARISATION AND SOFTWARE POLARISER FOR THE EISCAT UHF SYSTEM

Gudmund Wannberg

EISCAT HQ and IRF

December 2004, February 2009

Preface

Polarisation and polarisers have been causing EISCAT staff and users headaches ever since the first UHF operations in 1981. While the theory for how to compute the polarisation of the scattered signals at the receivers was well understood from the beginning, the electro-mechanical polarisers installed at the UHF remote sites have been a continual source of confusion and trouble. Whole EISCAT Technical Notes have been written on the subject of these polarisers and how best to calibrate them, internal reports have attempted to reconcile the commonly used polariser model with how the actual physical polariser behaves, and people have wrestled with the polariser phase and amplitude offsets and gotten them wrong half of the time. How many hours of data have been lost at the remote sites due to polariser-related problems is probably best left unmentioned… In spite of all these troubles, we have had to live with the old polarisers for more than two decades; there simply has been no alternative.

But during the last couple of years, the digital signal processing power installed at the Kiruna and Sodankylä sites has grown to a point that finally allows the polariser function to be implemented in real-time by software. A development polariser algorithm has recently been successfully tested and two extra receiver channels are now being constructed to allow routine operational use of the software polariser. As soon as these have been installed at the remote sites, the software-based system will permanently replace the old polarisers. Work is also in progress to add an adaptive capability that will make the polarisers essentially self-calibrating for the first time in EISCAT history, finally eliminating one of the most frequent and annoying sources of error encountered in multi-static operations. The experience gained from this project will be of direct relevance to the design of the planned EISCAT_3D advanced multi-static VHF radar system.

In the light of these developments, it is timely to revisit the theory and practice of wave polarisation and polarisers as used in EISCAT, the more so since all the early reports and notes discussing polariser-related matters are long since out of print and practically unobtainable. The present report attempts to cover the subject from basic theory to hardware and software implementation and verification. Borrowing heavily from the best standard textbooks on classical electrodynamics and radio astronomy wherever appropriate, it is intended both as an introduction to the subject for new users and staff as well as a reference document.

Kiruna, December 2004

Gudmund Wannberg

Revised version, published February 2009

Table of Contents:

1. Plane electromagnetic waves and wave polarisation

We begin by recalling some fundamentals of the theory of plane electromagnetic waves and define plane, circular and elliptical polarisations. For a comprehensive treatment the reader is referred to Chapter 7 of J. D. Jackson "Classical Electrodynamics" (1962, 1975).

In a source-free, loss-less infinite medium (e.g. vacuum), the solutions to Maxwell's equations are plane-wave fields of the form

$$\mathbf{E}\,(\mathbf{r},t) = \mathbf{E}\,\exp i(k\mathbf{n}\cdot\mathbf{r} - \omega t)$$
$$\mathbf{B}\,(\mathbf{r},t) = \mathbf{B}\,\exp i(k\mathbf{n}\cdot\mathbf{r} - \omega t) \qquad (1.1)$$

where $\mathbf{E}$, $\mathbf{B}$ and $\mathbf{n}$ are vectors that are constant in time and space. It can be shown (for the full treatment see Jackson p. 271) that under these conditions the only possible solutions are

$$\mathbf{E} = \mathbf{e}_1 E_1\,, \qquad \mathbf{B} = \mathbf{e}_2\sqrt{(\mu\varepsilon)}\,E_1 \qquad (1.2a)$$

or

$$\mathbf{E} = \mathbf{e}_2 E_2\,, \qquad \mathbf{B} = \mathbf{e}_1\sqrt{(\mu\varepsilon)}\,E_2 \qquad (1.2b)$$

where $\mathbf{e}_1$ and $\mathbf{e}_2$ are unit vectors orthogonal to $\mathbf{n}$ and to each other and the amplitude constants E_1 and E_2 are complex (Figure 1.1).

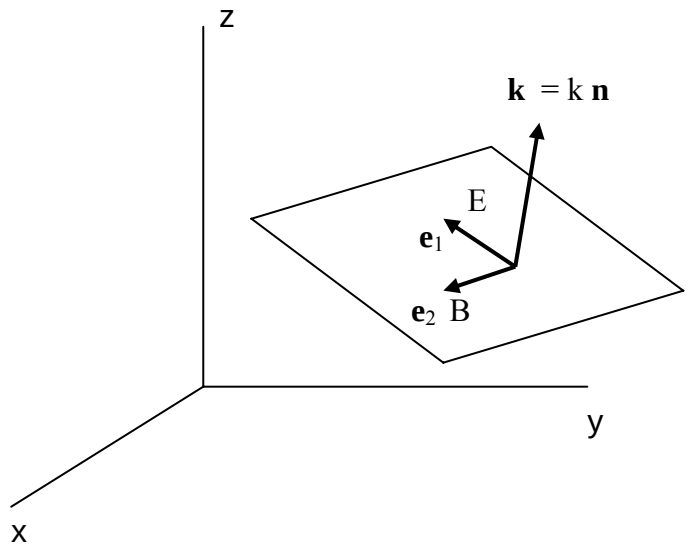

Figure 1.1: Propagation vector $\mathbf{k}$ and two orthogonal polarisation vectors $\mathbf{e}_1$ and $\mathbf{e}_2$ representing solutions 1.2a and 1.2 b

The electric field vector of the wave described by (1.2a) is always oriented in the $\mathbf{e}_1$ direction and the wave is said to be *linearly polarised* with polarisation vector $\mathbf{e}_1$. The wave described by (1.2b) is also linearly polarised with its polarisation vector oriented in the $\mathbf{e}_2$ direction, that is, orthogonal to $\mathbf{e}_1$, and the two solutions (1.2a) and (1.2b) are therefore linearly independent.

Linear combinations of the (1.2a) and (1.2b) solutions can be used to construct fields of all possible polarisation states. When both E_1 and E_2 are nonzero, the total time-varying electric field at a point **r** in space is given by:

$$\mathbf{E}\,(\mathbf{r},t) = [\mathbf{e}_1\,E_1 + \mathbf{e}_2\,E_2]\,\exp i(\mathbf{k}\cdot\mathbf{r} - \omega t) \qquad (1.3)$$

where in general both the magnitudes and the phases of E_1 and E_2 are different.

This wave is *elliptically polarised*. To understand what that means, let us first consider the special case that results when E_1 and E_2 have the same magnitude, E_0, but differ in phase by + or - $\pi/2$. Our wave then becomes

$$\mathbf{E}_{circ}(\mathbf{r},t) = E_0\,[\mathbf{e}_1 \pm i\,\mathbf{e}_2]\,\exp i(\mathbf{k}\cdot\mathbf{r} - \omega t) \qquad (1.4)$$

Without loss of generality we can rotate the (**e**$_1$ **e**$_2$ **n**) frame into alignment with the (**x y z**) one, such that the wave is propagating in the positive **z** direction while **e**$_1$ and **e**$_2$ are in the **x** and **y** directions, respectively. The x and y components of the physical electric field are then obtained by taking the real part of the realigned (1.3):

$$E_x(\mathbf{r},t) = \quad E_0 \cos(kz-\omega t) \qquad (1.5)$$
$$E_y(\mathbf{r},t) = \pm\, E_0 \sin(kz-\omega t)$$

At a fixed point in space, (0, 0, z), the field components given by (1.5) are such that the electric field vector $\mathbf{E}_{circ}$ is constant in magnitude but sweeps around **z** in a circle at an angular frequency ω; the wave is then said to be *circularly polarised.* $\mathbf{E}_{circ}$ can rotate in either direction. The two resulting counter-rotating fields are orthogonal:

$$\left|\,\mathbf{E}_{circ+}(\mathbf{r},t)\;\mathbf{E}_{circ-}(\mathbf{r},t)^*\,\right| = (1\cdot 1 - i\cdot(-i)) = 1 - 1 = 0$$

and they can therefore be used as a pair of basic fields, just as well as the (1.2a,b) pair.

We now return to (1.3) and introduce the complex amplitudes $E_{1'}$ and $E_{2'}$, which have different magnitudes and a $\pi/2$ phase difference. (1.4) and (1.5) then change into

$$\mathbf{E}_{ell}(\mathbf{r},t) = [E_{1'}\,\mathbf{e}_x \pm i\,E_{2'}\,\mathbf{e}_y]\,\exp i(\mathbf{k}\cdot\mathbf{r} - \omega t) \qquad (1.6)$$

$$E_x(\mathbf{r},t) = \quad E_{1'} \cos(kz-\omega t) \qquad (1.7a)$$
$$E_y(\mathbf{r},t) = \pm\, E_{2'} \sin(kz-\omega t) \qquad (1.7b)$$

$\mathbf{E}_{ell}$ also sweeps around at an angular frequency ω, just as $\mathbf{E}_{circ}$, but its magnitude varies with time. Putting z = 0 we get from (1.7a)

$$\cos(-\omega t) = E_x(t) / E_{1'} \quad \text{and so} \quad \sin(-\omega t) = \sqrt{\{1 - [E_x(t) / E_{1'}]^2\}}$$

Introducing this into (1.7b) and rearranging terms gives:

$$[E_x(t) / E_{1'}]^2 + [E_y(t) / E_{2'}]^2 = 1 \qquad (1.8)$$

which is the *equation of an ellipse with half-axes* $E_{1'}$ *and* $E_{2'}$ oriented along **x** and **y**, respectively. Thus, as ωt goes through the full 2π, $\mathbf{E}_{ell}$ traces out an ellipse and this is the reason why the wave described by (1.6) is said to be *elliptically polarised*.

When $\angle E_{1'} \neq \angle E_{2'} \pm \pi/2$ the polarisation ellipse is tilted with respect to the x and y axes. In the limit of $\angle E_{1'} = \angle E_{2'}$ it collapses into a line through the origin. $\mathbf{E}_{ell}$ then describes a linearly-polarised wave with its plane of polarisation oriented at an angle $\beta = \text{atan}\,(E_{2'}/E_{1'})$ to the **x** axis.

We can use this to rewrite Eq. (1.6) a little. Rather than specifying the magnitudes of the two complex amplitudes explicitly, they can be expressed as fractions of the root-mean-square amplitude vector $\mathbf{E_0}$:

$$\mathbf{E_0} \cos\beta = |E_{1'}| \qquad \text{and} \qquad \mathbf{E_0} \sin\beta = |E_{2'}|$$

It is obviously possible to make $E_{1'}$ and $E_{2'}$ take on any values by varying $\mathbf{E_0}$ and β, so this is a valid (and as we will show later, convenient for our purposes) substitution. If we also introduce the phase angle δ explicitly, (1.6) changes into

$$\mathbf{E_0}(\mathbf{r},t) = \mathbf{E_0}\,(\mathbf{e}_x \cos\beta + \mathbf{e}_y \sin\beta \exp i\delta) \exp i(\mathbf{k}\cdot\mathbf{r} - \omega t) \qquad (1.9)$$

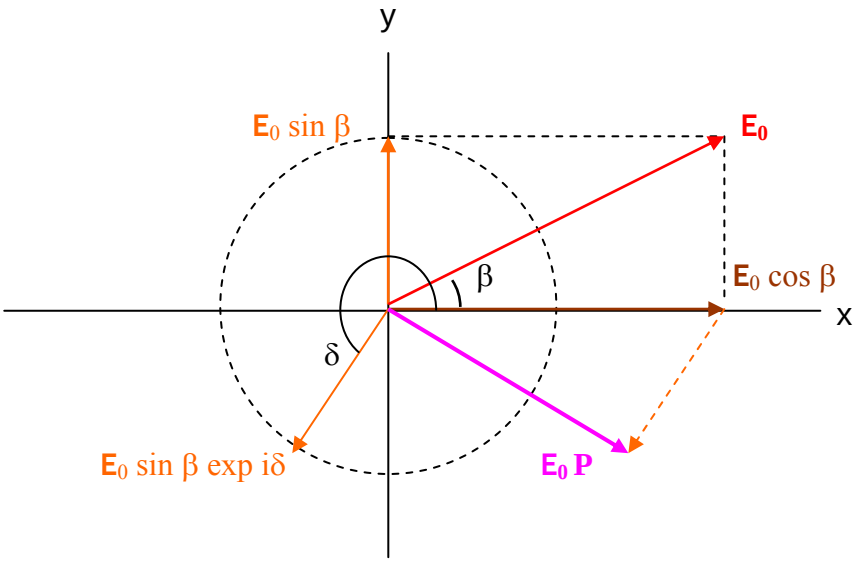

Figure 1.2: Showing how two complex-valued component amplitude vectors with magnitudes $E_0 \cos\beta$ and $E_0 \sin\beta$ add up to form a composite amplitude vector $E_0 P$. In this example the phase angle δ is approximately 240°. Note that when $\delta = \pm 90°$, $E_0 P = E_0$ [cos β, ± sin β]

(1.9) can be rearranged into *vector format*:

$$\mathbf{E_0} = \mathbf{E_0} \begin{bmatrix} \cos\beta \\ \\ \sin\beta \exp i\delta \end{bmatrix} \exp i(\mathbf{k}\cdot\mathbf{r} - \omega t) \quad = \mathbf{E_0}\,\mathbf{P} \exp i(\mathbf{k}\cdot\mathbf{r} - \omega t) \qquad (1.10)$$

which expresses $\mathbf{E_0}$ as a product of three separate and independent quantities:

- A *magnitude* $\mathbf{E_0}$,
- a *polarisation vector* **P**, and
- a *space-time factor* exp i(**k**·**r** - ωt).

Note that **P** is fully specified by the two angles β and δ !

Using the **P** notation, the polarisation properties of the four basic fields that we have been looking at above can be expressed in a very compact form:

$$\mathbf{P} = \begin{bmatrix} 1 \\ 0 \end{bmatrix} \quad \Longleftrightarrow \quad \text{linear polarisation along the x axis} \qquad \text{(cf. 1.2a)}$$

$$\mathbf{P} = \begin{bmatrix} 0 \\ 1 \end{bmatrix} \quad \Longleftrightarrow \quad \text{linear polarisation along the y axis} \qquad \text{(cf. 1.2b)}$$

$$\mathbf{P} = (1/\sqrt{2}) \begin{bmatrix} 1 \\ +\,i \end{bmatrix} \quad \Longleftrightarrow \quad \text{right circular polarisation}$$

$$\mathbf{P} = (1/\sqrt{2}) \begin{bmatrix} 1 \\ -\,i \end{bmatrix} \quad \Longleftrightarrow \quad \text{left circular polarisation} \qquad \text{(cf. 1.5)}$$

2. Scattering of electromagnetic waves – and how their polarisation is affected

We now consider how an EM wave is scattered by a single electron and how the polarisation of the scattered wave depends on the scattering geometry. Refer to Figure 2.1.

An electron is located at point O in vacuum, far away from other matter and charges. An incident EM wave with wave vector $\mathbf{k}_0$, generated by a radar transmitter located at T, sets up a periodic electric field **E**(t) at the location of the electron:

$$\mathbf{E}(t) = \mathrm{Re}\,(\mathbf{E_0} \exp(-i\,\omega_0 t)) \qquad (2.1)$$

The force exerted on the electron by **E**(t) causes it to describe a harmonic oscillation:

$$-e\,\mathbf{E}_0 \exp(-i\,\omega_0 t) = m_e \,.\, d\mathbf{v}_e/dt \qquad (2.2)$$

The motion of the point electric charge on the electron sets up a time-varying current that induces a secondary electromagnetic field, which re-radiates ("scatters") the power intercepted from the incident wave. A receiver located at R observes a scattered wave with wave vector $\mathbf{k_1}$. Following Hagfors (1975) we now investigate the detailed relation between $\mathbf{E}_0$ and $\mathbf{E}_1$. Refer to Figure 2.1.

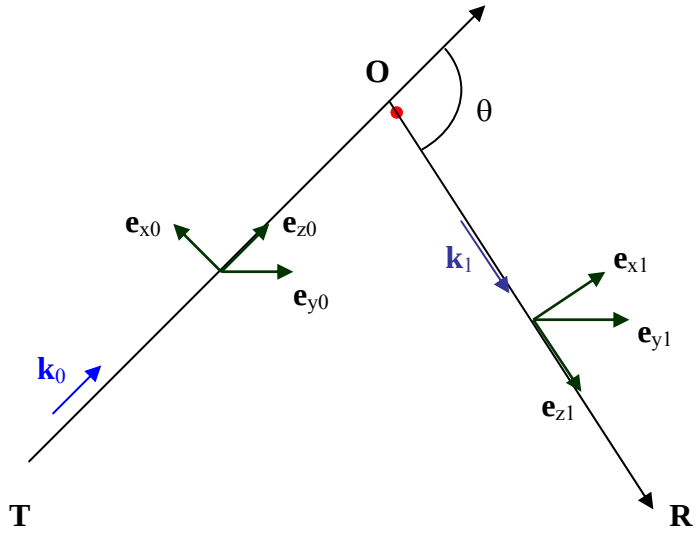

Figure 2.1: Coordinate systems used for the definition of the state of polarisation of the scattered EM wave

$\mathbf{k}_0$ and $\mathbf{k}_1$ lie in a plane through **T**, **O** and **R**. θ is the *scattering angle*, i.e. the angle in the plane between $\mathbf{k}_0$ and $\mathbf{k}_1$. We introduce two right-handed Cartesian bases, ($\mathbf{e}_{x0}$ $\mathbf{e}_{y0}$ $\mathbf{e}_{z0}$) and ($\mathbf{e}_{x1}$ $\mathbf{e}_{y1}$ $\mathbf{e}_{z1}$):

$\mathbf{e}_{z0}$ and $\mathbf{e}_{z1}$ are aligned with $\mathbf{k}_0$ and $\mathbf{k}_1$ respectively,
$\mathbf{e}_{y0}$ and $\mathbf{e}_{y1}$ are normal to the plane through $\mathbf{k}_0$ and $\mathbf{k}_1$, and
$\mathbf{e}_{x0}$ and $\mathbf{e}_{x1}$ are oriented so as to complete the bases.

Since EM waves are transverse waves with **E** and **B** normal to their wave vector, only the component of $\mathbf{E}_0$ normal to $\mathbf{k_1}$ excites the scattered wave:

$$\mathbf{E}_1 = \mathbf{E}_0 \; |\, \mathbf{k_1} \times \mathbf{E}_0 \,| \,/\, (|\, \mathbf{k_1} \,| \,.\, |\mathbf{E}_0\,|) = \mathbf{E}_0 \sin \chi \qquad (2.3)$$

where χ is the the *polarisation angle*. This means that in terms of our two Cartesian bases, the y component of $\mathbf{E}_0$ maps unchanged onto the y component of $\mathbf{E}_1$, but only a cos θ - fraction of the x-component of $\mathbf{E}_0$ maps onto the x-component of $\mathbf{E}_1$.

Using (1.10) we can express the polarisation $\mathbf{P}_1$ and magnitude $\mathbf{E_1}$ of the scattered wave as:

$$\mathbf{E_1}\,\mathbf{P}_1 = K\,\mathbf{E_0} \begin{bmatrix} \cos\theta & 0 \\ 0 & 1 \end{bmatrix} \mathbf{P}_0 \qquad (2.4)$$

where K is a proportionality constant. This determines the relationship of the two fields. In particular we note (the proof is left to the reader as an exercise) that

$$\sin^2 \chi = \sin^2 \beta_0 + \cos^2 \beta_0 \cos^2 \theta \qquad (2.5)$$

Three specific combinations of incident polarisation and scattering geometry are particularly interesting from a practical point of view:

1) When the incident wave is linearly polarised along $\mathbf{e}_{y0}$, the scattered wave is also linearly polarised along $\mathbf{e}_{y1}$ and $\sin^2 \chi = 1$ independently of θ,

2) If the incident wave is linearly polarised along $\mathbf{e}_{x0}$, the scattered wave is also linearly polarised along $\mathbf{e}_{x1}$, but in this case $\sin^2 \chi = \cos^2 \theta$, so that for scattering through $\theta = 90^o$, $\sin^2 \chi$ becomes = 0 and $\mathbf{E}_1$ vanishes !

3) When the incident wave is circularly polarised, i.e. when $\sin \beta_0 = \cos \beta_0 = 1/\sqrt{2}$ and $\delta = 90^o$, we have

$$\mathbf{P}_1 = (1/\sqrt{2}) \begin{bmatrix} \cos\theta \\ i \end{bmatrix}$$

In this case a signal backscattered towards the transmitter ($\theta = 180^o$) is also circularly polarised with $\sin^2 \chi = 1$ – but its sense of rotation is reversed relative to the incident wave, since $\cos 180^o = -1$. When the scattering is through 90^o, the $\mathbf{e}_{x0}$ part of the incident wave is aligned with $\mathbf{k}_1$ and the scattered signal is linearly polarised along $\mathbf{e}_{y1}$ with $\sin^2 \chi = ½$. That is, at any given distance from the scatterer, the signal power that can be recovered after scattering through 90^o is only half of that available after backscattering through 180^o.

3. Faraday rotation

So far all wave propagation has been assumed to take place in a homogeneous, isotropic medium. But in the ionosphere, this no longer holds -

The plasma in the ionosphere is magnetized by the Earth's magnetic field. This makes it *birefringent* and *anisotropic* to propagating electromagnetic waves. A full treatment of the associated wave propagation theory is beyond the scope of the present report, but Jackson Section 7.6 provides an easy-to-understand qualitative description. A somewhat more stringent treatment can be found in Kraus, Chapter 5.4.

The core issue here is that the theory shows that in a magnetised plasma, EM waves can only propagate in either of two orthogonal eigenmodes, viz. a left-handed circularly polarised (LHC) mode or a right-handed circularly polarised (RHC) mode, and ε_+ *and* ε_-, *the effective dielectric constants for the two modes, are unequal.*

For propagation parallel to the local magnetic field:

$$\varepsilon_\pm = 1 - \omega_p^2 / [\omega (\omega \pm \omega_B)] \qquad (3.1)$$

where ω_p^2 is the *plasma frequency* (which to first order is proportional to the square root of the electron density) and and ω_B is the *electron gyrofrequency* (which is proportional to the magnetic field strength).

Accordingly, $\eta_\pm$, *the refractive indices* for the LHC and RHC modes, are also different:

$$\eta_\pm = \sqrt{\mu}\ \sqrt{\varepsilon_\pm} \tag{3.2}$$

The *phase constants* of the two modes, i.e. their rates of phase progression per unit path length, are $\beta_\pm$:

$$\beta_\pm = \omega / v_\pm = \omega\eta_\pm / c \tag{3.3}$$

Now consider what happens when a linearly polarised EM wave is incident on magnetised plasma. Since linear polarisation is not an eigenmode in the plasma, this wave must be treated as the resultant of one LHC wave and one RHC wave of equal magnitude. As these propagate, they accumulate phase $\theta_\pm$ at slightly different rates:

$$d(\theta_+ - \theta_-) = (\beta_+ - \beta_-)\, dr \tag{3.4}$$

The absolute phase angle of the resultant linearly-polarised wave, θ, will therefore change at half that rate:

$$d\theta = \tfrac{1}{2}(\beta_+ - \beta_-)\, dr \tag{3.5}$$

which shows that *in a magnetised plasma the polarisation plane of a linearly polarised wave rotates as the wave propagates* ! This effect is known as *Faraday rotation*.

When $\omega > \omega_p$, $\omega >> \omega_B$, $\sqrt{\mu} \cong 1$ and ϕ (the angle between the magnetic field and the propagation direction) $\leq 60^o$, $(\beta_+ - \beta_-)$ can be approximated by

$$\beta_+ - \beta_- = (\omega / c)\,(\omega_p^2\, \omega_B \cos\phi / \omega^3) \tag{3.6}$$

Using the familiar expressions for ω_p^2 and ω_B:

$$\omega_p^2 = n_e\, e^2 / (\varepsilon_0\, m_e) \quad \text{and} \quad \omega_B = B\, e / m_e$$

we obtain the so-called *quasi-longitudinal approximation* to the differential phase:

$$d\theta \cong e^3\, n_e\, B \cos\phi\, dr / (2\, \omega^2\, c\, \varepsilon_0\, m_e^2) \tag{3.7}$$

The total Faraday rotation along a ray path is then obtained by integration:

$$\theta = e^3 / (2\, \omega^2\, c\, \varepsilon_0\, m_e^2) \int n_e(r)\, B(r) \cos\phi(r)\, dr \tag{3.8}$$

Now we are finally in a position to make some numerical estimates. As an example we compute the Faraday rotation suffered by a linearly polarised radar wave going up along the

local magnetic field line, from the ground up to the peak of the F layer at 300 km altitude and back, under typical ionospheric conditions:

From 200 km to 300 km altitude, we assume an average electron density, $n_e \approx 1.2 \cdot 10^{11}$ m^{-3}. From 200 km down to the bottom of the E layer the density is lower, typically around $1 \cdot 10^{10}$ m^{-3}. Below the E layer we can consider the atmosphere to be unionised. B can be put approximately equal to $5 \cdot 10^{-5}$ Tesla over the whole altitude range. For a one-way trip from the ground to 300 km, this results in a rotation

$$\theta\ (0 - 300\text{km}) \approx 1.32 \cdot 10^{18}\ \omega^{-2}$$

which for $\omega = 2\pi \cdot 930$ MHz (the approximate operating frequency of the EISCAT UHF system) becomes ≈ 0.044 radians or about 2.5 degrees.

On its way down the scattered wave will suffer an equal and additional amount of rotation – *Faraday rotation is cumulative*. At 930 MHz this still makes the total rotation only some five degrees, just about enough to be noticeable.

But Faraday rotation is inversely proportional to frequency squared, so at the EISCAT VHF frequency (224 MHz) the total rotation becomes about 86 degrees! If a common linearly polarised antenna is used both for transmission and for reception, it will recover only $\sin^2$ (90-86) or 0.48 % of the signal power – *for this particular electron density profile the Faraday rotation causes the* VHF *echo signal from* 300 *km to vanish* ! At VHF, linear polarisation is obviously a poor choice for any monostatic ionospheric radar application.

The logical (and optimal) choice is circular polarisation. Which of the two senses, LHC or RHC, to use for transmission is unimportant; both are eigenmodes in the plasma and the handedness will change in the scattering process anyway, such that an upgoing LHC wave will come down as RHC and vice versa.

4. Signal polarisation in the UHF system

The UHF antenna at Tromsø can transmit any chosen polarisation – linear, circular or elliptical. However, since the very beginning it has been set up to employ RHC/LHC polarisation. While not strictly necessary for avoiding Faraday rotation effects, this is technically and operationally expedient. The waveguide *orthomode transformer* (OMT) that separates the RHC and LHC modes provides better than - 20 dB of isolation between its two ports, which aids greatly in protecting the receiver from the megawatt-level transmitter pulses. Circular polarisation also provides the Kiruna and Sodankylä receive-only sites with a reasonably balanced illumination in all look directions over the entire tri-static field of view.

As configured at present (December 2004) the UHF system transmits a RHC polarised signal. All signals received at Tromsø are backscattered through 180^o and therefore LHC polarised, irrespective of where the Tromsø antenna is pointing (cf. Section 2, special case 3).

On the other hand, signals transmitted from Tromsø and received at the Kiruna and Sodankylä sites are scattered through scattering angles θ_{TK} and θ_{TS} determined by the pointing geometry of any particular experiment and always smaller than 180^o, approximately as shown in Figure 2.1. *These signals are therefore always elliptically polarised* (cf. Eq. 2.4). The ellipticity and

tilt of their polarisation ellipses are functions of the position of the common scattering volume, and so the receiving antennas must have a *continuously variable polarisation response* in order to always put all the intercepted scattered power into a single signal.

Equation 1.9 suggests one way to accomplish this in practice. Expanded like this:

$$\mathbf{E_0}(\mathbf{r},t) = \mathbf{E_0} \cos\beta \exp i(\mathbf{k}\cdot\mathbf{r} - \omega t) + \mathbf{E_0} \sin\beta \exp i\delta \exp i(\mathbf{k}\cdot\mathbf{r} - \omega t) \qquad (4.1)$$

it shows that any EM wave is the vector sum of two phase-coherent, spatially orthogonal, linearly polarised component waves whose amplitude ratio and relative phase are fully determined by the angles β and δ. Therefore, *if the antenna system is set up to respond to two orthogonal linear polarisations simultaneously, the two corresponding component signal voltages represent two independent parts of the signal power, which together contain all information about* $\mathbf{E_0}$. *It is always possible to rotate one of the signal components until it is orthogonal to the other (recall that both are complex vectors!) and add them, which recovers* $\mathbf{E_0}$. In this way, the polarisation-matching problem can be reduced to two sub-tasks, viz. how to separate incoming waves into two orthogonal component waves and how to process and recombine the signal voltages into a common signal. We shall now see how this is done in the EISCAT UHF system.

Figure 4.1 illustrates how an incoming plane wave propagates through one of the receive-only UHF antennas. The reflector system is a so-called Cassegrain geometry; the plane wave enters the reflector system along the optical axis of the antenna, ***Z***, reflects off the paraboloidal primary reflector, onto the hyperboloidal secondary reflector and from there into a circular feedhorn, located such that its phase center coincides with the focal point of the secondary reflector image. Since both reflectors are surfaces of revolution and axially symmetric around the optical axis, the antenna is polarisation-insensitive up to this point and the wave polarisation is conserved.

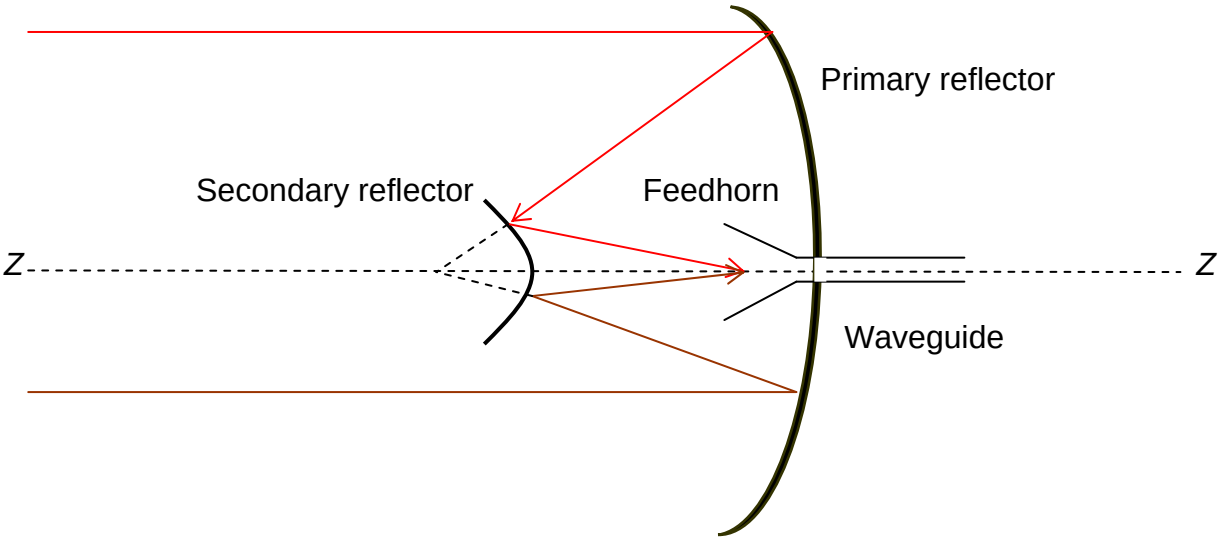

Figure 4.1: Schematic illustration of the reflector system of a Cassegrain radio telescope. The ray paths of two incoming paraxial rays (representing different parts of a plane wave field) are indicated in red and brown.

Leaving the horn, the wave travels through a short piece of circular waveguide and then enters an *orthomode transformer* (OMT). Figure 4.2 shows a photograph of the Kiruna OMT. This is a three-port waveguide network that has a square input port with a side length equal to the diameter of the horn mouth. A short distance from the input port, the square waveguide branches out into two rectangular, 2:1 aspect ratio waveguides, oriented at right angles to each other. The upper (***H***) waveguide is oriented such that its **E** field is aligned with the local horizontal (and the antenna elevation axis), while the **E** field in the lower (***V***) waveguide is normal to both ***H*** and ***Z***. The ***H*** and ***V*** waveguides and the optical axis of the antenna thus define a local Cartesian system that is fixed with respect to the antenna and moves with it as its pointing direction is changed. This system can be specified by a set of unit vectors $\mathbf{e}_H$, $\mathbf{e}_V$ and $\mathbf{e}_Z$. The ***V*** waveguide is often sloppily referred to as the "vertical" one, but this is true only when the antenna points towards the horizon – at all other times its **E** field is off-vertical.

Since the polarisation of the transmitted wave and the geographical locations of the UHF sites are known, the values of β and δ in the ($\mathbf{e}_H$ $\mathbf{e}_V$ $\mathbf{e}_Z$) system can be computed for any given bi-static pointing geometry by vector algebra. Software routines that do this are integrated into the antenna control software package. The Faraday rotation suffered by the scattered wave between the scattering point and the receiving site is usually neglected.

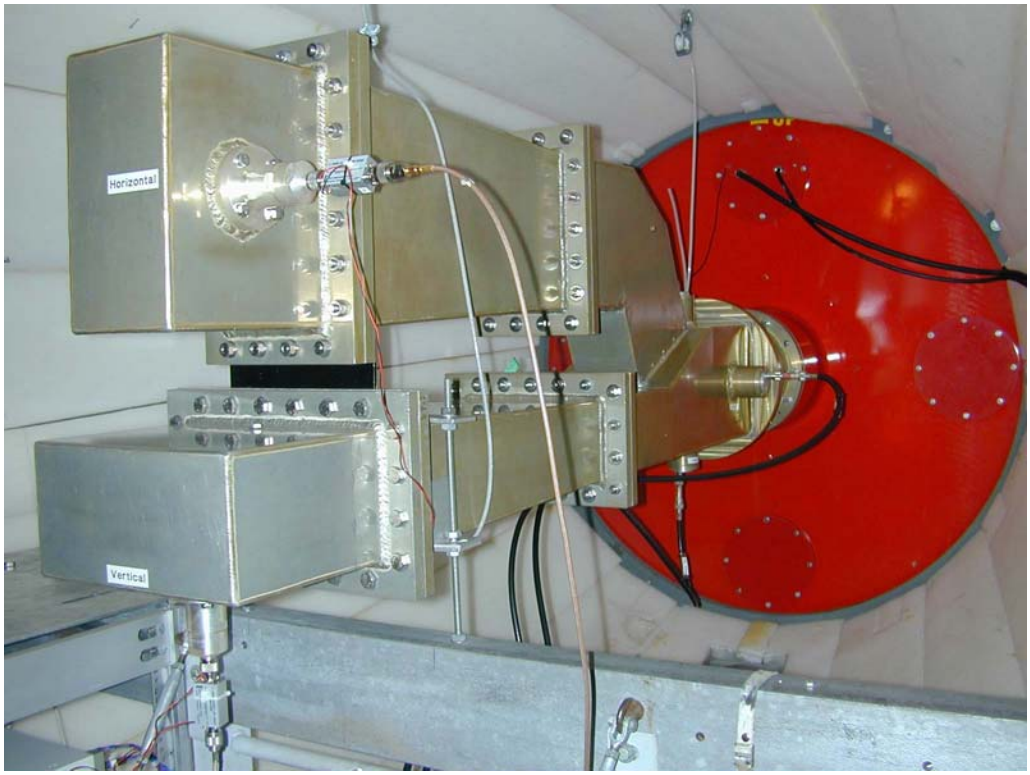

Figure 4.2: A UHF orthomode transformer (Kiruna site).

Since the ***H*** and ***V*** waveguides support only the dominant TE_{10} mode at 930 MHz, the component of the incoming wave whose **E** field points in the $\mathbf{e}_H$ direction will propagate only in the upper waveguide, but not in the lower one. Similarly, the component whose **E** field points in the $\mathbf{e}_V$ direction will propagate only in the lower waveguide, but not in the upper one. In this way the incident EM wave is separated into two linearly polarised, spatially orthogonal component waves, aligned with $\mathbf{e}_H$ and $\mathbf{e}_V$ – exactly what we need!

Both waveguides end in waveguide-to-coax transitions, which extract the signal power and impedance-transform it to the nominally 50+j0 ohm preamplifier imput impedance. The preamplifiers are the small boxes attached to the ends of the large coaxial lines that can be seen sticking out from the waveguides.

Since losses in the OMT are negligible, the signal energy is conserved in the transformation from free space conditions to the 50-ohm system, and the input signal voltage amplitudes $U_{H,V}$ therefore become

$$U_{H,V} = E_{H,V} \cdot (2 \cdot 50/377)^{½} \approx 0.52\ E_{H,V} \qquad (4.2)$$

The preamplifiers amplify the input signal voltages by some factor G, producing two time-varying output voltages H(t) and V(t):

$$H(t) = G\ U_H \cos\ \omega t \qquad (4.3)$$

$$V(t) = G\ U_V \cos(\omega t + \phi_{VH}) \qquad (4.4)$$

where ϕ_{VH} is the relative phase between the two signals. G is assumed to be the same in both channels.

At this point it is convenient to go over into complex vector representation; since H(t) and V(t) have been derived from two spatially orthogonal plane-polarised components of the received signal, they can be interpreted as the real and imaginary components of a *vector voltage* $\mathbf{U}_S(t)$ representing the total flow of signal power from antenna to load:

$$\mathbf{U}_S(t) = \begin{bmatrix} G\ U_H \cos(\omega t) \\ G\ U_V \cos(\omega t + \phi_{VH}) \end{bmatrix} = G \cdot \mathrm{Re}\left[\begin{bmatrix} U_H \\ U_V \exp \mathbf{i}\ \phi_{VH} \end{bmatrix} \exp \mathbf{i}\ (\omega t) \right] \qquad (4.5)$$

This is in almost the same as our old friend Eq. 1.10, but with a twist:

$$\begin{bmatrix} U_H \exp -\mathbf{i}\ \phi_0 \\ U_V \exp -\mathbf{i}\ \phi_0 \end{bmatrix} = (U_S / G) \exp -\mathbf{i}\ \phi_0 \begin{bmatrix} \cos \beta \\ \sin \beta \exp \mathbf{i}\ \delta \exp \mathbf{i}\ \Theta_0 \end{bmatrix} \qquad (4.6)$$

We recognize the matrix in the right-hand member of (4.6), $\mathbf{P}_{\Theta 0}$, as the polarisation matrix **P** of the received wave with an extra phase factor exp **i** Θ_0 in the vertical branch:

$$\phi_{VH} = \Theta_0 + \delta$$

That is, the relative phase ϕ_{VH} is the sum of the free-space relative phase δ and an extra term Θ_0 that accounts for the net difference in electrical length between the V and H signal paths - Fig. 4.2 shows clearly that the lengths of the V and H waveguides coming out of the OMT are quite different!

If we now introduce an extra phase advance $d\Theta = 90^o - \delta - \Theta_0$ into the V signal path or an equivalent phase delay $-d\Theta$ into the H path, the total receiver phase becomes $\Theta = \Theta_0 + d\Theta = 90^o - \delta$, which makes $\phi_{VH} = 90^o$ and causes the H and V signals U_H and $U_{V\Theta}$ to end up in phase quadrature.

The vector voltage $\mathbf{U}_{S\perp}(t)$ formed by U_H and $U_{V\Theta}$ contains all the signal power, such that on average:

$$P_{S\Sigma} = <\mathbf{U}_{S\perp}(t)^2> / Z_0 \qquad = < (U_H(t)^2 + U_{V\Theta}(t)^2) > / Z_0 \qquad (4.7)$$

where the brackets denote ensemble averaging and Z_0 is the load impedance.

In an ideal, noise-free situation we could have stopped here – a simple time delay or vector rotation is all it would take to recover the total signal power. Unfortunately, in the real world, all measurements of physical quantities are noise-corrupted to a greater or lesser degree, so we must next consider how to recover the information from a weak signal competing with noise.

5. Noise, scatter signals and signal-to-noise ratio (SNR)

Noise in a radio-receiving system is both of external and internal origin. It is often convenient to relate the amount of noise seen by the system to an interface right at the receiver input and express it in terms of an *equivalent noise temperature* T_N. The famous *Nyqvist noise formula* states that the noise power delivered by a resistive generator at absolute temperature T into a matched resistive load is equal to

$$P = k\,T\,B \qquad (5.1)$$

where k is Boltzmann's constant and B is the measurement bandwidth. If we assume that the receiver is matched to the antenna and B is known, T_N can be computed as:

$$T_N = P_N / (kB) \qquad (5.2)$$

Each of the two orthogonal channels of an EISCAT UHF (930 MHz) remote receiver exhibits an overall T_N of about 40 - 50 K. This is state-of-the-art and about as low as one can hope to achieve on a regular basis at 930 MHz. About 10 - 15 K of the total noise is due to radiation from deep space picked up through the antenna main lobe. Some 5 K is due to thermal radiation from the ground picked up through the sidelobes. The rest, 15 – 25 K, is internal receiver noise, generated partly in loss resistances in transmission lines and impedance matching networks and partly by non-thermal noise generator mechanisms intrinsic to the preamplifier. Because the receiver H and V channels are physically independent, the noise generated internally in one channel is uncorrelated with that generated in the other channel. The external noise is also largely uncorrelated between two channels, since at 930 MHz most of the deep sky noise picked up by the antenna is unpolarised. Therefore, to a very good approximation the noise voltages out of the H and V channels are uncorrelated on average.

We now study the case of a scatter signal co-existing with noise in the dual polarisation EISCAT UHF receiver. To simplify matters, we consider only the spectral power in the angular frequency interval (ω,ω+dω). The results can later be expanded to any desired spectral interval.

The noise voltage components associated with the (ω,ω+dω) interval are

$$U_{NH} \exp(i\omega) \quad \text{and} \quad U_{NV} \exp(i\omega)$$

By restricting ourselves to the interval (ω,ω+dω) we can discard the exp (iω) Fourier factor and retain only the complex amplitudes.

In each channel, the noise voltage (which corrupts the information) and the scatter signal voltage (which contains the information we are after) add to form the *noise-corrupted composite channel voltages* $\mathbf{U}_H$ and $\mathbf{U}_V$:

$$\mathbf{U}_H = \mathbf{U}_{SH} + \mathbf{U}_{NH} \qquad \text{and} \qquad \mathbf{U}_V = \mathbf{U}_{SV} + \mathbf{U}_{NV} \tag{5.3}$$

where $\mathbf{U}_{SH}$ and $\mathbf{U}_{SV}$ are defined by Eq. 4.5. As explained above, U_{NH} and U_{NV} are uncorrelated on average:

$$< U_{NH} U_{NV}^* > = 0 \tag{5.4}$$

All permutations of the scatter signals and the noise components are also uncorrelated:

$$< U_{SH} U_{NH}^* > = < U_{SV} U_{NV}^* > = < U_{SH} U_{NV}^* > = < U_{SV} U_{NH}^* > = 0 \tag{5.5}$$

so in the following analysis it is okay to treat signal and the noise as independent.

In most incoherent scatter radar measurement situations the noise – sadly – dominates over the signal. For instance, in the EISCAT UHF system SNR is frequently < 0.1, particularly during the midwinter when the ionosphere above northern Scandinavia is in darkness and the electron density drops to a very low value. Under these conditions, the statistical accuracy of a measurement is basically proportional to the *signal-to-noise ratio*, SNR:

$$\text{SNR} = P_S / P_N \tag{5.6}$$

where P_S is the average signal power and P_N the ensemble average power of the stochastic noise corrupting the measurement.

To obtain optimum statistics from our dual polarisation receiver, we want to arrange matters such that the ratio P_S / P_N maximises. Intuitively, one might think that this happens automatically if we combine the signal voltages $\mathbf{U}_{SH}$ and $\mathbf{U}_{SV}$ from the two receiver channels into a voltage signal that contains all the signal power P_S.

But it is not as simple as that. The recombination of $\mathbf{U}_{SH}$ and $\mathbf{U}_{SV}$ can be done in several different ways and *not all of them automatically maximise SNR !* To demonstrate this, we now investigate two different approaches in detail.

The first is a direct application of Eqs. 4.6 and 4.7. Only the composite voltages $\mathbf{U}_H$ and $\mathbf{U}_V$ are directly accessible in the receiver, but we can bring the $\mathbf{U}_{SV}$ component of $\mathbf{U}_V$ into quadrature with the $\mathbf{U}_{SH}$ component of $\mathbf{U}_H$ by rotating $\mathbf{U}_V$ through Θ:

$$\mathbf{R}(\Theta)\mathbf{U}_V = \mathbf{R}(\Theta)\mathbf{U}_{SV} + \mathbf{R}(\Theta)\mathbf{U}_{NV} = \mathbf{U}_{SV\Theta} + \mathbf{U}_{NV\Theta} \tag{5.7}$$

$$\mathbf{U}_{\Sigma\Theta} = \mathbf{U}_H + \mathbf{R}(\Theta)\mathbf{U}_V \qquad (\mathbf{U}_{SV\Theta} \perp \mathbf{U}_{SH}) \tag{5.8}$$

The total power carried by the sum vector voltage $\mathbf{U}_{\Sigma\Theta}$ can be estimated by squaring it, taking the norm and dividing by the load impedance Z_0:

$$P_\Sigma = <|\mathbf{U}_{\Sigma\Theta}(t)^2|> / Z_0 = <|(\mathbf{U}_{SH} + \mathbf{U}_{SV\Theta})^2|> / Z_0 + <|(\mathbf{U}_{NH} + \mathbf{U}_{NV\Theta})^2|> / Z_0 \tag{5.9}$$

In analogy with Eq. 4.7, the first term in the RHM now contains all signal power:

$$<|(\mathbf{U}_{SH} + \mathbf{U}_{SV\Theta})^2|> / Z_0 = P_{S\Sigma} \tag{5.10}$$

But the noise components $\mathbf{U}_{NH}$ and $\mathbf{U}_{NV\Theta}$ are uncorrelated and have arbitrary phase angles γ_H and $\gamma_{V\Theta}$:

$$\gamma_{V\Theta} = \gamma_H + \pi/2 + \psi \tag{5.11}$$

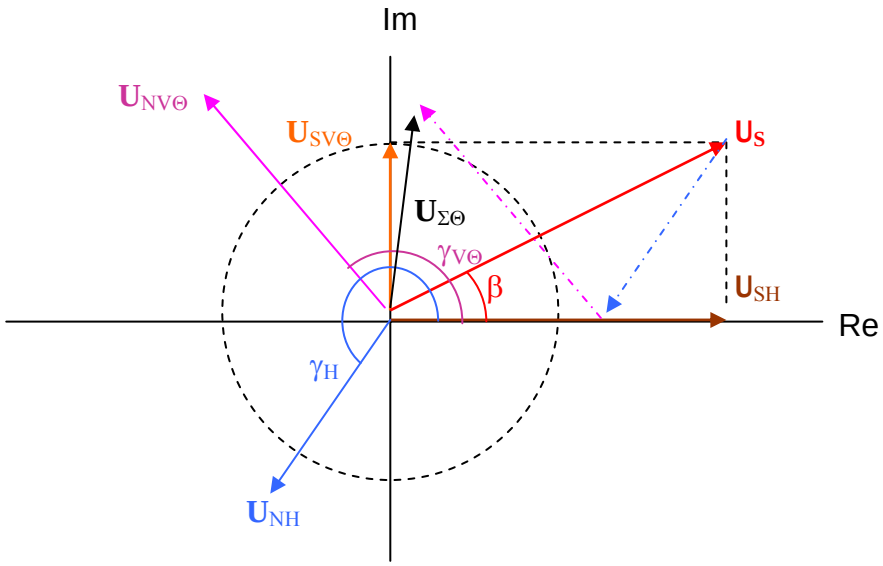

Figure 5.1: Rotating $\mathbf{U}_V$ through Θ causes the two signal voltage components $\mathbf{U}_{SH}$ and $\mathbf{U}_{SV\Theta}$ to become orthogonal. In the case illustrated here, they also happen to line up with the Re and Im axes of our complex voltage reference system. On the other hand, the two uncorrelated noise voltage components $\mathbf{U}_{NH}$ and $\mathbf{U}_{NV\Theta}$ are in arbitrary phases also after the rotation. The sum vector voltage $\mathbf{U}_{\Sigma\Theta} = \mathbf{U}_S + \mathbf{U}_{NH} + \mathbf{U}_{NV\Theta}$ is shown in black.

The vector sum of $\mathbf{U}_{NH}$ and $\mathbf{U}_{NV\Theta}$ is $\mathbf{U}_{N\Sigma}$:

$$\mathbf{U}_{N\Sigma} = \begin{bmatrix} \text{Re } \mathbf{U}_{N\Sigma} \\ \\ \text{Im } \mathbf{U}_{N\Sigma} \end{bmatrix} = \begin{bmatrix} U_{NH} \cos \gamma_H - U_{NV} \sin (\gamma_H + \psi) \\ \\ U_{NH} \sin \gamma_H + U_{NV} \cos (\gamma_H + \psi) \end{bmatrix} \quad (5.12)$$

and the total noise power, $P_{N\Sigma}$, is

$$P_{N\Sigma} = < \text{Re}^2 \mathbf{U}_{N\Sigma} + \text{Im}^2 \mathbf{U}_{N\Sigma} > / 2 Z_0 \quad (5.13)$$

But $< \text{Re}^2 \mathbf{U}_{N\Sigma} + \text{Im}^2 \mathbf{U}_{N\Sigma} > =$

$$= U_{NH}^2 + U_{NV}^2 - 2 U_{NH} U_{NV} <\cos \gamma_H \sin (\gamma_H + \psi) + \sin \gamma_H \cos (\gamma_H + \psi)>$$

$$= U_{NH}^2 + U_{NV}^2 \text{ (because the ensemble average term vanishes)} \quad (5.14)$$

leading to

$$P_\Sigma = P_{S\Sigma} + (U_{NH}^2 + U_{NV}^2) / 2 Z_0 \quad (5.15)$$

which shows that, in addition to the total signal power, P_Σ also contains *all the noise power from both the* H *channel and the* V *channel* !

This is bad news. We know that if the scatter signal received by the antenna is horizontally polarised, i.e.$\beta = 0$, all the signal power is contained in the U_{SH} component. In that case, the signal-to-noise ratio (SNR) in the H channel is

$$SNR_H = (U_{SH} / U_{NH})^2 \quad (5.16)$$

But:

$$SNR_\Sigma = U_{SH}^2 / (U_{NH}^2 + U_{NV}^2) < SNR_H \quad (5.17)$$

If the noise temperatures of the H and V channels are about equal, then $U_{NH} \cong U_{NV}$ =>

$$SNR_\Sigma \cong 0.5 \, SNR_H \quad (5.18)$$

The situation is comparable for a vertically polarised scatter signal ($\beta = 1$). In fact, a little algebra shows that the SNR will suffer for any arbitrary polarisation; merely vector adding the H and V channel signals and squaring the sum vector results in a *decrease* of the SNR, not an increase! This is clearly not what we set out to achieve…

But - *with a clever extra bit of vector manipulation we can effectively remove about half of the noise power at the same time as we extract all the signal power* -

Since $\mathbf{U}_{SV\Theta} \perp \mathbf{U}_{SH}$, it follows that $-\mathbf{U}_{SV\Theta} \perp \mathbf{U}_{SH}$ and $|(\mathbf{U}_{SH} + \mathbf{U}_{SV\Theta})| = |(\mathbf{U}_{SH} - \mathbf{U}_{SV\Theta})|$. The total signal power can therefore be recovered either as:

$$P_{S\Sigma} = \mathbf{U}_{S\Sigma}^2 / 2 Z_0 = | (\mathbf{U}_{SH} + \mathbf{U}_{SV\Theta})^2 | / 2 Z_0 \quad (5.19a)$$

or as

$$P_{S\Delta} = \mathbf{U}_{S\Delta}^2 / 2\,Z_0 = \left| \left(\mathbf{U}_{SH} - \mathbf{U}_{SV\Theta}\right)^2 \right| / 2\,Z_0 \qquad (5.19b)$$

The phase angle between $\mathbf{U}_{S\Delta}$ and $\mathbf{U}_{S\Sigma}$ is 2β. Therefore, if we form a difference vector $\mathbf{U}_{\Delta\Theta}$:

$$\mathbf{U}_{\Delta\Theta} = \mathbf{U}_H - \mathbf{R}(\Theta)\mathbf{U}_V \qquad (5.20)$$

in analogy with the procedure in (5.5) and (5.6) and then rotate $\mathbf{U}_{\Sigma\Theta}$ through $-\beta$ and $\mathbf{U}_{\Delta\Theta}$ through $+\beta$, the signal parts of the rotated vectors $\mathbf{R}(-\beta)\,\mathbf{U}_{\Sigma\Theta}$ and $\mathbf{R}(+\beta)\,\mathbf{U}_{\Delta\Theta}$ will be aligned.

Consequently,

$$\begin{aligned}
&\left|\left(\mathbf{R}(-\beta)\,\mathbf{U}_{\Sigma\Theta} + \mathbf{R}(+\beta)\,\mathbf{U}_{\Delta\Theta}\right)^2\right| = \\
&\quad = \left|\left(\mathbf{R}(-\beta)\,\mathbf{U}_{N\Sigma} + \mathbf{R}(+\beta)\,\mathbf{U}_{N\Delta}\right)^2\right| + \left|\left(2\,\mathbf{U}_{S\Sigma}\right)^2\right| \\
&\quad = \left|\left(\mathbf{R}(-\beta)\,\mathbf{U}_{N\Sigma} + \mathbf{R}(+\beta)\,\mathbf{U}_{N\Delta}\right)^2\right| + \left|\left(2\,\mathbf{U}_{S\Delta}\right)^2\right| \\
&\quad = \left|\left(\mathbf{R}(-\beta)\,\mathbf{U}_{N\Sigma} + \mathbf{R}(+\beta)\,\mathbf{U}_{N\Delta}\right)^2\right| + 4\left|\mathbf{U}_{S\Sigma}^2\right| \\
&\quad = \left|\left(\mathbf{R}(-\beta)\,\mathbf{U}_{N\Sigma} + \mathbf{R}(+\beta)\,\mathbf{U}_{N\Delta}\right)^2\right| + 4\left|\mathbf{U}_{S\Delta}^2\right| \qquad (5.21)
\end{aligned}$$

This shows that the signal power can be extracted from $[\mathbf{R}(-\beta)\,\mathbf{U}_{S\Sigma} + \mathbf{R}(+\beta)\,\mathbf{U}_{S\Delta}]$ just as well as from $\mathbf{U}_{S\Sigma}$ or $\mathbf{U}_{S\Delta}$, apart from a scale factor equal to 4.

$\mathbf{U}_{N\Delta}$, the noise part of $\mathbf{U}_{\Delta\Theta}$ is

$$\mathbf{U}_{N\Delta} = \begin{bmatrix} \mathrm{Re}\,\mathbf{U}_{N\Delta} \\ \mathrm{Im}\,\mathbf{U}_{N\Delta} \end{bmatrix} = \begin{bmatrix} U_{NH}\cos\gamma_H + U_{NV}\sin\left(\gamma_H + \psi\right) \\ U_{NH}\sin\gamma_H - U_{NV}\cos\left(\gamma_H + \psi\right) \end{bmatrix} \qquad (5.22)$$

and the vector sum of $\mathbf{U}_{N\Sigma}$ and $\mathbf{U}_{N\Delta}$ after the rotation through $\pm\beta$ becomes:

$$\mathbf{R}(-\beta)\,\mathbf{U}_{N\Sigma} + \mathbf{R}(+\beta)\mathbf{U}_{N\Delta} = 2 \begin{bmatrix} U_{NH}\cos\beta\cos\gamma_H + U_{NV}\sin\beta\sin\left(\gamma_H + \psi\right) \\ U_{NH}\sin\beta\sin\gamma_H - U_{NV}\cos\beta\cos\left(\gamma_H + \psi\right) \end{bmatrix} \qquad (5.23)$$

leading to

$$\begin{aligned}
&\left|\left(\mathbf{R}(-\beta)\,\mathbf{U}_{N\Sigma} + \mathbf{R}(+\beta)\,\mathbf{U}_{N\Delta}\right)^2\right| = \\
&= 4\,\{\,U_{NH}^2\cos^2\beta + U_{NV}^2\sin^2\beta + \\
&\quad + U_{NH}\,U_{NV}\cos\beta\sin\beta\,\langle\cos\gamma_H\cos\left(\gamma_H + \psi\right) - \sin\gamma_H\sin\left(\gamma_H + \psi\right)\rangle\,\} \qquad (5.24)
\end{aligned}$$

Since γ_H and ψ are random variables,

$$\int < \ldots > d\gamma_H = \int < \ldots > d\psi = 0$$

and (5.20) reduces to

$$< \left| (\mathbf{R}(-\beta)\, \mathbf{U}_{N\Sigma} + \mathbf{R}(+\beta)\, \mathbf{U}_{N\Delta})^2 \right| > = 4 \{ U_{NH}^2 \cos^2 \beta + U_{NV}^2 \sin^2 \beta \} \qquad (5.25)$$

Thus the noise power in the $\mathbf{R}(-\beta)\, \mathbf{U}_{\Sigma\Theta} + \mathbf{R}(+\beta)\, \mathbf{U}_{\Delta\Theta}$ *signal is a weighted sum of noise from the* H *channel and the* V *channel, with the weighting factors* $\cos^2 \beta$ *and* $\sin^2 \beta$ *proportional to the relative fractions of signal power carried by the* H *and* V *signal voltage components*, such that for a horizontally polarised signal ($\beta = 0$) all the noise comes from the H channel and $SNR_{\Sigma+\Delta} = SNR_H$. Similarly, for a vertically polarised signal ($\beta = 1$) $SNR_{\Sigma+\Delta} = SNR_V$.

But if the noise temperatures of the H and V channels are nearly equal,

$$<U_{NH}> \cong <U_{NV}> \cong U_{N0} \qquad (5.26)$$

and because $(\cos^2 \beta + \sin^2 \beta) = 1$ for all β, (5.21) further reduces to

$$< \left| (\mathbf{R}(-\beta)\, \mathbf{U}_{N\Sigma} + \mathbf{R}(+\beta)\, \mathbf{U}_{N\Delta})^2 \right| > \cong 4 <U_{NH}^2> \cong 4<U_{NV}^2> \cong 4\, U_{N0}^2 \qquad (5.27)$$

That is, *when the noise temperatures of the two channels are close to equal, the total noise power is equal to the noise power from either channel, independently of the value of* β !

So this approach procedures exactly the result we want – for any pair of angles (Θ,β) the sum voltage vector

$$\mathbf{U}_{\Sigma opt} = \mathbf{R}(-\beta)\, \mathbf{U}_{\Sigma\Theta} + \mathbf{R}(+\beta)\, \mathbf{U}_{\Delta\Theta} \qquad (5.28)$$

contains all the scatter signal power and at the same time provides optimum signal-to-noise ratio. Now all that remains to do is to find a practical way of generating it…

Since $\mathbf{U}_{\Sigma opt}$ is formed by a sequence of vector rotations and vector summations, realising it in practice means that $\mathbf{U}_H$ and $\mathbf{U}_V$ (or processed replicas of them) have to be passed through a cascade of phase-shifters and adders. These can be either hardware devices operating directly on the RF signal, or software routines operating in the digital domain. From the point of view of the subsequent signal processing the two approaches are equivalents, but which one we choose will have a dramatic impact on the receiver architecture!

When the first EISCAT UHF receivers were constructed in the 1970s, there was not really a choice. At that time, real-time digital signal processing was difficult and extremely costly and radar receivers were generally designed to pre-process the received signals as much as possible at RF or IF, before the A/D conversion, in order to reduce the DSP requirements. At EISCAT, this philosophy produced the *analogue polariser,* a coaxial network containing two motor-driven "trombone" phase shifters and two four-port hybrids. After pre-amplification,

the 930 MHz $\mathbf{U}_H(t)$ and $\mathbf{U}_V(t)$ RF signals enter the network and by setting the phase shifters appropriately, $\mathbf{U}_{\Sigma opt}$ and $\mathbf{U}_{\Delta opt}$ can be made to emerge at the two output ports.

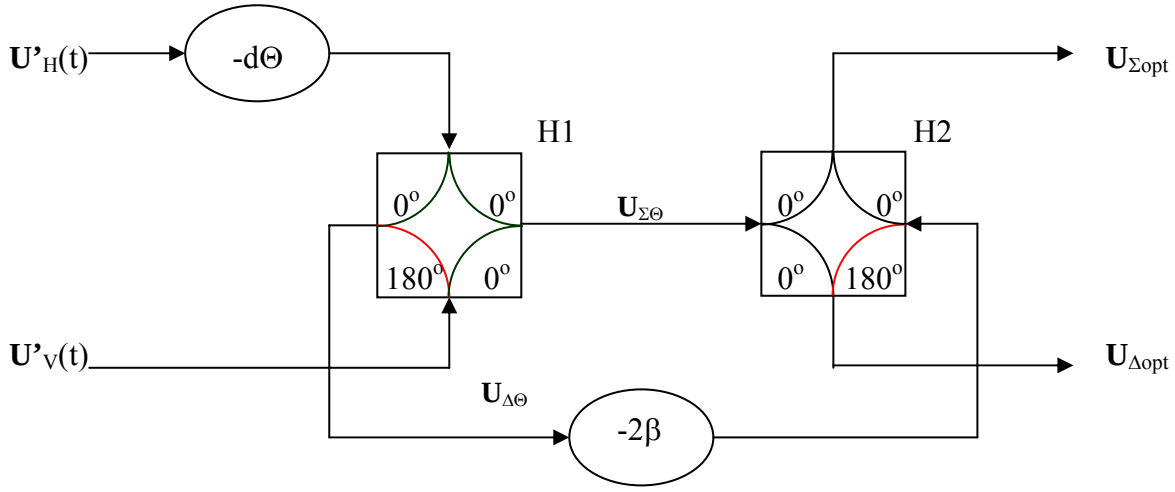

Figure 5.1: Schematic diagram of the EISCAT UHF analogue polariser. The elements marked -dΘ and -2β are the motor-driven "trombone" phase shifters. H1 and H2 are four-port 180° hybrids, summing networks that generate the sum and difference of two input signals.

The -dΘ phase shifter retards $\mathbf{U'}_H(t)$ by the correct amount to bring the two signals into quadrature at the H1 inputs. H1 then generates $\mathbf{U}_{\Sigma\Theta}$ and $\mathbf{U}_{\Delta\Theta}$ according to Eqs. 5.8 and 5.20. Finally, the -2β phase shifter and H2 recombine $\mathbf{U}_{\Sigma\Theta}$ and $\mathbf{U}_{\Delta\Theta}$ into $\mathbf{U}_{\Sigma opt}$ and $\mathbf{U}_{\Delta opt}$. The adjustment range of the dΘ and -2β phase shifters is > 360°. Note that these can only delay a signal but never advance its phase and so must sometimes be set modulo 360°.

Figure 5.2: Photograph of the EISCAT UHF analogue polariser. The oblong gray objects are the motor-driven "trombone" phase shifters. The small boxes at the left-hand end of the phase shifters contain the four-port 180° hybrids H1 and H2.

6. The UHF receiver and the software polariser algorithm

A software polariser is essentially a piece of software that accepts processed replicas of $\mathbf{U}_H$ and $\mathbf{U}_V$ appearing at the radar receiver output as inputs, evaluates Eqs. 5.8, 5.20 and 5.28 using pre-computed values for the expected amplitude ratio (tan β) and the phase angle δ, and outputs $\mathbf{U}_{\Sigma opt}$ (or a scaled replica of it).

A prerequisite to implementing a software polariser is obviously that there are two separate signal paths through the receiver, all the way from the antenna to the computer input buffer, such that $\mathbf{U}_H$ and $\mathbf{U}_V$ can be processed independently of each other. Hardware is now (early 2005) being added to the Kiruna and Sodankylä UHF receiver systems to provide the required second channel.

When a signal **v** passes through a receiver channel, its characteristics are modified. The relationship between the input signal **v** and the output signal **V** is described by the channel *transfer function* $\mathcal{H}$**:**

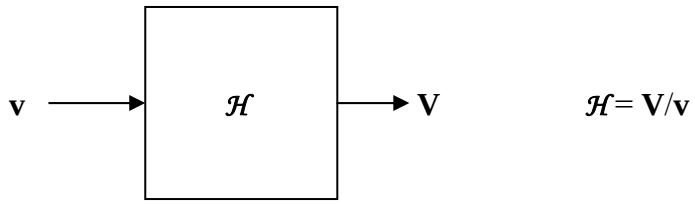

Due to component and manufacturing tolerances, the transfer functions $\mathcal{H}_H$ and $\mathcal{H}_V$ of the two UHF receiver channels are always unequal to some degree. This is normal, considering that the total channel gain is in the order of 100 dB, but it causes the gain and phase relationship between the channel output signals to be different from that existing between $\mathbf{U}_H$ and $\mathbf{U}_V$. The receiver output signals must therefore be re-normalised before Eqs. 5.8, 5.20 and 5.28 can be evaluated correctly using the pre-computed values for (tan β) and δ.

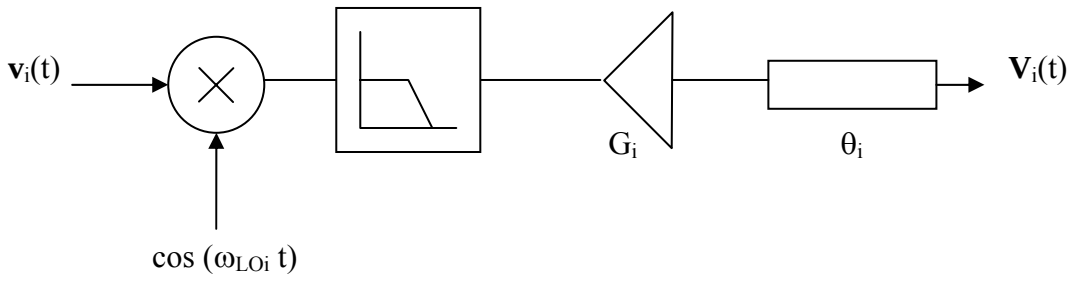

Figure 6.1: Model of a receiver channel. The functional blocks in the signal path are, from left to right, a *mixer*, a *filter*, an *amplifier* and a *delay line*. i = (H,V).

The "analogue" part of a receiver channel (i.e. the part from the antenna terminals to the A/D converter input) can be modelled as a cascade of four functional blocks, viz. a *mixer,* a *filter,* an *amplifier* and a *delay line* (Figure 6.1). The mixer and filter blocks are assumed to be

lossless and delay-free, while all gains and losses are bundled into the amplifier block and all phase delays are bundled into the delay line block.

- An input signal $\mathbf{v}_i(t) = v_i \cos(\omega t + \phi_i)$ enters the *mixer* where it is multiplied with a monochromatic signal at the *local oscillator frequency* ω_{LOi}. This operation produces a new signal with spectral components ("sidebands") at the sum frequency $(\omega+\omega_{LOi})$ and the difference frequency $(\omega-\omega_{LOi})$.
- The *filter* passes only the difference sideband at $(\omega-\omega_{LOi})$. In this way the information contained in $\mathbf{v}_i$ is translated downwards in the frequency domain,
- The *amplifier* raises the amplitude of the translated signal, $\frac{1}{2} v_i \cos((\omega-\omega_{LOi})t + \phi_i)$, by some *channel gain factor* G_i,
- Finally, the *delay line* delays the amplified signal, $\frac{1}{2} G_i v_i \cos((\omega-\omega_{LOi})t + \phi_i)$, by some *phase delay* θ_i

The analogue channel transfer function can therefore be expressed as:

$$\mathcal{H}_i = \frac{1}{2} G_i \left\{ \frac{\cos(\theta_i + \phi_i)\ \cos(\omega - \omega_{LOi})\, t}{\cos(\omega t + \phi_i)} + \frac{\sin(\theta_i + \phi_i)\ \sin(\omega t - \omega_{LOi})\, t}{\cos(\omega t + \phi_i)} \right\} \quad (6.1)$$

This model is *amplitude and phase linear*, that is, G_i and θ_i are constants and not functions of v_i, ω or ϕ_i. In the UHF receiver, both channels derive their local oscillator signals from a common oscillator unit, i.e. $\omega_{LO(H)} = \omega_{LO(V)} = \omega_{LO}$. This automatically maintains relative phase coherency between the channels. *Gain* and *phase inequalities* between the channels will manifest themselves however. If a monochromatic, unity amplitude signal with frequency ω_{LO} and zero initial phase,

$$\mathbf{v}_0(t) = \cos \omega_{LO} t,$$

is injected into both the H channel and the V channel, the output signals $\mathbf{V}_H(t)$ and $\mathbf{V}_V(t)$ become:

$$\mathbf{V}_H(t) = \frac{1}{2} G_H \{\cos \theta_H + \sin \theta_H\} \quad (6.2)$$

and

$$\mathbf{V}_V(t) = \frac{1}{2} G_V \{\cos \theta_V + \sin \theta_V\} \quad (6.3)$$

Since $G_H \neq G_V$ and $\theta_H \neq \theta_V$ in general $\rightarrow \mathbf{V}_H \neq \mathbf{V}_V$

By adding a *phase delay equalisation term* Ω to Eq. 6.3 and multiplying it by a *gain equalisation factor* Γ we can generate a "corrected $\mathbf{V}_V$ " signal:

$$\mathbf{V}^C_V = \frac{1}{2} \Gamma G_V \{\cos(\theta_V + \Omega) + \sin(\theta_V + \Omega)\} \quad (6.4)$$

Putting $\Gamma = G_H / G_V$

and $\Omega = \Delta\theta = \theta_H - \theta_V$ leads to

$$\mathbf{V}^C_V = \tfrac{1}{2}\, G_V\, (G_H / G_V)\, \{\cos(\theta_V + (\theta_H - \theta_V)) + \sin(\theta_V + (\theta_H - \theta_V))\}$$

or $$\mathbf{V}^C_V \equiv \mathbf{V}_H \qquad (6.5)$$

We leave it as an exercise for the reader to show that this procedure (a rotation through $\Omega = \Delta\theta$ followed by a multiplication by $\Gamma = G_H / G_V$) will re-normalise the output signal pair resulting from any two input signals.

Before the software can take over, $\mathbf{V}_H$ and $\mathbf{V}_V$ must first be converted from real-valued to complex-valued and digitised. In the physical UHF receiver this is done as follows:

In the analogue channels, the 930 MHz RF signals are translated down to an *intermediate frequency* (i.f.) band at (11.25 +/-3) MHz. The band-limited, real-valued channel output signals $\mathbf{V}_H(t)$ and $\mathbf{V}_V(t)$ are sampled synchronously at 15 Msamples/second by a Pentek 3420 dual channel A/D converter unit. The two sample streams are then *digitally down-converted to complex baseband* by multiplication with a complex-valued periodic sequence, *low-pass filtered* to select the difference frequency components and limit their power spectral content to a narrow region around zero frequency (typically some ± 25 kHz, just wide enough to accommodate a single ion-acoustic scatter spectrum), and finally *decimated*. After the decimation we are left with a pair of low-rate (≈100 ksamples/second), complex-valued time series sample streams, $\mathbf{S}_H(n\tau)$ and $\mathbf{S}_V(n\tau)$, which replicate the instantaneous amplitude values of the spectral components passed by the digital low-pass filters.

The mapping of $\mathbf{V}_H$ and $\mathbf{V}_V$ into $\mathbf{S}_H$ and $\mathbf{S}_V$ is amplitude and time linear and affects the channel transfer functions only by contributing a multiplicative complex scaling factor. This is however exactly the same for both channels, such that $\mathbf{S}_H(n\tau)$ and $\mathbf{S}_V(n\tau)$ retain the same relative phase and amplitude relationship as $\mathbf{V}_H(t= n\tau)$ and $\mathbf{V}_V(t= n\tau)$.

Consequently, *the polariser function can be implemented by applying the channel gain and phase re-normalisation procedure of* Eq. 6.4 *to* $\mathbf{S}_V(n\tau)$ *and using the resulting series of sample pairs* ($\mathbf{S}_H$, $\mathbf{S}^C_V$) *as input to* Eqs. 5.8, 5.20 *and* 5.28*!*

The prototype polariser software now being tested does not implement each equation explicitly but merges some computing operations to gain speed:

1) Firstly, $\mathbf{S}_V$ is gain-equalised and at the same time its signal component is brought into phase quadrature with the signal component of $\mathbf{S}_H$:

   If the phase difference between $\mathbf{U}_V$ and $\mathbf{U}_H$ at the receiver input is

   $$\phi_{VH} = \Theta_0 + \delta$$

   where Θ_0 is the antenna/feed-system phase difference and δ the polarisation phase angle, and if the differential phase delay between the H and V receiver channels is

   $$\Delta\theta = \theta_H - \theta_V$$

then the net phase difference between $\mathbf{V}_V$ and $\mathbf{V}_H$ at the ADC input (and therefore also between $\mathbf{S}_V$ and $\mathbf{S}_H$) is

$$\Psi = \angle (\mathbf{V}_V, \mathbf{V}_H) = \phi_{VH} + \Delta\theta$$

Rotating $\mathbf{S}_V$ in the positive sense through $\phi_{PH} = \pi/2 - \Psi$ therefore brings the signal components of the two sample vectors into phase quadrature. To equalise the gains, the components of the rotated $\mathbf{S}_V$ must then be multiplied by Γ. In matrix notation:

$$\begin{bmatrix} \text{Re } \mathbf{S}_V' \\ \text{Im } \mathbf{S}_V' \end{bmatrix} = \Gamma \begin{bmatrix} \cos\phi_{PH} & -\sin\phi_{PH} \\ \sin\phi_{PH} & \cos\phi_{PH} \end{bmatrix} \begin{bmatrix} \text{Re } \mathbf{S}_V \\ \text{Im } \mathbf{S}_V \end{bmatrix}$$

or

$$\mathbf{S}_V' = \Gamma\, \mathbf{R}(\phi_{PH}) * \mathbf{S}_V$$

where $\mathbf{R}$ is the *rotation operator*.

But because Γ and ϕ_{PH} normally remain constant over many (> thousands) sample pairs - ϕ_{PH} changes only when δ changes as a result of an antenna pointing change and Γ changes appreciably only on time scales of hours or more - we can reduce the number of multiply operations by forming a *composite correction matrix* $\mathbf{R}_\Gamma(\phi_{PH})$, which is recomputed only when necessary (e.g. following an antenna pointing change):

$$\mathbf{R}_\Gamma(\phi_{PH}) = \begin{bmatrix} \Gamma\cos\phi_{PH} & -\Gamma\sin\phi_{PH} \\ \Gamma\sin\phi_{PH} & \Gamma\cos\phi_{PH} \end{bmatrix}$$

This reduces the real-time computation in this step to a single matrix operation:

$$\mathbf{S}_V' = \mathbf{R}_\Gamma(\phi_{PH}) * \mathbf{S}_V$$

which encapsulates the whole of Eq. 6.4 and the vector rotation part of Eq. 5.8. See Figure 6.2a.

2) Intermediate sum and difference vectors $\mathcal{V}_I$ and $\mathcal{V}_{II}$ are formed (Figure 6.2b):

$$\mathcal{V}_I = \mathbf{S}_H + \mathbf{S}_V'$$
$$\mathcal{V}_{II} = \mathbf{S}_H - \mathbf{S}_V'$$

3) $\mathcal{V}_{II}$ is then rotated in the positive sense through 2β to generate $\mathcal{V}_{II}'$ (Figure 6.2c):

$$\mathcal{V}_{II}' = \mathbf{R}(2\beta) * \mathcal{V}_{II}$$

Obviously, $|\mathcal{V}_{II}'| = |\mathcal{V}_{II}|$

Rotating $\mathcal{V}_{II}$ through 2β rather than rotating $\mathcal{V}_I$ and $\mathcal{V}_{II}$ through -β and +β as in Eq. 5.28 reduces the number of multiply operations in this step from eight to four. This is in analogy with the old hardware polariser that also uses only a single "trombone" phase shifter to implement this step.

4) Finally, $\mathcal{V}_\Sigma = \mathcal{V}_I + \mathcal{V}_{II}'$ and $\mathcal{V}_\Delta = \mathcal{V}_I - \mathcal{V}_{II}'$ are formed (Eq. 5.28 and its complement).

One consequence of the computational shortcut in step 3 is that the absolute phases of $\mathcal{V}_\Sigma$ and $\mathcal{V}_\Delta$ are advanced by +β relative to what they would have been if Equation 5.28 had been implemented explicitly, but this is unimportant in all normal incoherent scatter applications – absolute phase does not affect a power spectral estimate.

If optimal numerical values of β, δ, Γ, Θ_0 and Δθ have been used throughout the procedure, the signal part of $\mathcal{V}_\Delta$ should now vanish and the signal part and signal-to-noise ratio of $\mathcal{V}_\Sigma$ should maximise. $\mathcal{V}_\Sigma$ is transferred to the lag_wrap input buffer; the $\mathcal{V}_\Sigma$ (t) time series becomes the input vector for all subsequent DSP computations.

On the other hand, if one or more parameter values are not optimum, $\mathcal{V}_\Sigma$ does <u>not</u> maximise and $\mathcal{V}_\Delta$ does <u>not</u> vanish; this can be exploited both when calibrating the system initially and eventually to make the polariser algorithm adaptive.

Figure 5.2a: Rotating $\mathbf{S}_{VS}$ into phase quadrature with $\mathbf{S}_{HS}$

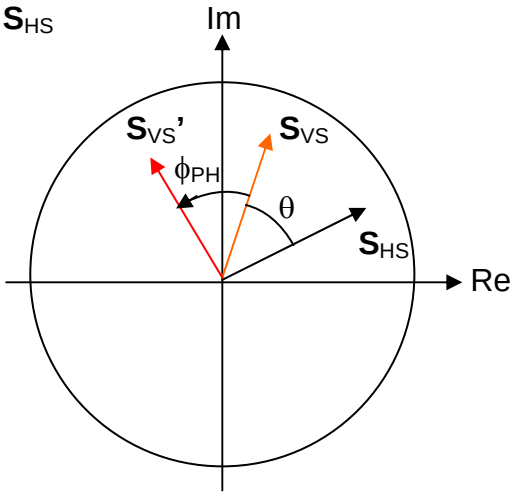

Figure 5.2b: Forming sum and difference vectors $\mathcal{V}_{I\,S}$ and $\mathcal{V}_{II\,S}$

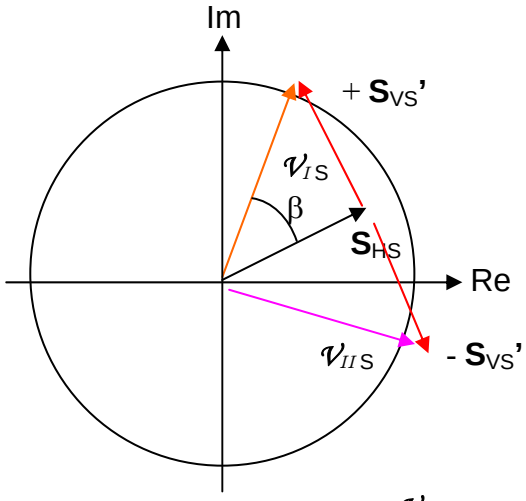

Figure 5.2c: Rotating $\mathcal{V}_{II\,S}$ into alignment with $\mathcal{V}_{I\,S}$ and forming $\mathcal{V}_{\Sigma S}$, $\mathcal{V}_{\Delta S}$